DNA Breaks-Mediated Fitness Cost Reveals RNase HI as a New Target for Selectively Eliminating Antibiotic-Resistant Bacteria

Roberto Balbontín,* Nelson Frazão, and Isabel Gordo*
Instituto Gulbenkian de Ciência, Oeiras, Portugal

*Corresponding authors: E-mails: rbalbontin@igc.gulbenkian.pt; igordo@igc.gulbenkian.pt.
Associate editor: Miriam Barlow

Abstract

Antibiotic resistance often generates defects in bacterial growth called fitness cost. Understanding the causes of this cost is of paramount importance, as it is one of the main determinants of the prevalence of resistances upon reducing antibiotics use. Here we show that the fitness costs of antibiotic resistance mutations that affect transcription and translation in *Escherichia coli* strongly correlate with DNA breaks, which are generated via transcription–translation uncoupling, increased formation of RNA–DNA hybrids (R-loops), and elevated replication–transcription conflicts. We also demonstrated that the mechanisms generating DNA breaks are repeatedly targeted by compensatory evolution, and that DNA breaks and the cost of resistance can be increased by targeting the RNase HI, which specifically degrades R-loops. We further show that the DNA damage and thus the fitness cost caused by lack of RNase HI function drive resistant clones to extinction in populations with high initial frequency of resistance, both in laboratory conditions and in a mouse model of gut colonization. Thus, RNase HI provides a target specific against resistant bacteria, which we validate using a repurposed drug. In summary, we revealed key mechanisms underlying the fitness cost of antibiotic resistance mutations that can be exploited to specifically eliminate resistant bacteria.

Key words: **antibiotic resistance, fitness cost, DNA breaks, RNase HI targeting, repurposed drug.**

Article

Introduction

Antibiotic resistance entails a large health and economic burden worldwide (World Health Organization 2018). Its maintenance and spread in bacterial populations depend on the rate at which resistance is acquired and on its effect on bacterial fitness. This effect is typically deleterious in the absence of antibiotics, resulting in the so-called cost of resistance (Melnyk et al. 2015; Vogwill and MacLean 2015). The fitness cost of resistance is influenced by the environment, by interactions between the resistances and the genetic background in which they appear (epistasis), and by subsequent acquisition of mutations compensating for fitness defects (compensatory evolution) (Durão et al. 2018). Importantly, the magnitude of the cost is one of the main parameters influencing the fate of resistances upon reducing antibiotic use (Andersson and Hughes 2010). Despite its importance, the causes of the fitness cost of resistance are far from being completely understood (Vogwill and MacLean 2015), and the identification of factors affecting the cost of resistance is an important issue in the fields of antibiotic resistance and public health.

Resistance mutations often map to genes encoding proteins targeted by antibiotics. These target proteins are involved in essential functions, such as transcription, translation, DNA replication, or cell wall biosynthesis. Resistance mutations cause alterations in the biochemical properties of the target protein, rendering it insensitive to the drug, but often adversely affecting its function (Andersson and Levin 1999; Andersson and Hughes 2010; Durão et al. 2018). These pleiotropic effects hold the key to manipulating resistance levels in bacterial populations (Andersson and Hughes 2010). Rifampicin and streptomycin resistance mutations (Rif^R and Str^R) are representative examples of resistances to antibiotics targeting transcription and translation commonly found in pathogenic bacteria (Eliopoulos 1993; Lemos and Matos 2013; Goldstein 2014). These resistances map to the genes *rpoB* and *rpsL*, encoding the β subunit of the RNA polymerase and the protein S12 of the 30S ribosomal subunit, respectively. Rif^R mutations show different fitness costs (Jin and Gross 1989; Reynolds 2000) and cause alterations in the rates of transcription initiation, elongation, slippage, or termination (Das et al. 1978; Guarente and Beckwith 1978; Yanofsky and Horn 1981; Gowrishankar and Pittard 1982; Fisher and Yanofsky 1983; Hammer et al. 1987; Jin, Cashel, et al. 1988; Jin, Walter, et al. 1988; Jin and Gross 1989, 1991; Jin and Zhou 1996; Zhou and Jin 1997, 1998; Reynolds 2000; Zhou et al. 2013). Likewise, most Str^R mutations also cause a cost (Ruusala et al. 1984; Schrag and Perrot 1996; Paulander et al. 2009) and affect translation fidelity and processivity (Gorini and Kataja 1964; Gartner and Orias 1966; Birge and Kurland 1969; Ozaki et al. 1969; Galas and Branscomb 1976; McMahon and Landau 1982; Bohman et al. 1984; Dong and Kurland 1995; Schrag and Perrot 1996;

Paulander et al. 2009). Thus, defects in protein synthesis, either at a global cellular level (Applebee et al. 2008; Hall et al. 2011; Qi et al. 2014) or limited to specific functions or regulons (Zhou and Jin 1998; Paulander et al. 2009; Ochi and Hosaka 2013; Pelchovich et al. 2014) are important causes for the fitness costs of Rif^R and Str^R mutations.

Recently, we observed that compensatory evolution of costly double-resistant mutants (Rif^R Str^R) resulted in overexpression of *nusG* or *nusE* (Moura de Sousa et al. 2017), which encode the proteins that physically connect the RNA polymerase and the ribosome (Burmann et al. 2010). This finding suggests that additional factors, alongside altered protein synthesis, contribute to the fitness cost of these resistances. Specifically, it raises the possibility of cost reduction occurring via reinforcement of the coupling between transcription and translation by increasing the amounts of NusE and NusG (Moura de Sousa et al. 2017), implying that Rif^R and Str^R mutations can generate transcription–translation uncoupling. Importantly, Rif^R and Str^R mutations have been shown to affect the coordination between these processes (Jensen 1988; Elgamal et al. 2016). Coupling between transcription and translation and NusG function are both known to prevent spontaneous backtracking of the RNA polymerase (retrogressive sliding along DNA and RNA) which, if excessive, can cause a series of molecular events that ultimately lead to the generation of double-strand DNA breaks (Herbert et al. 2010; Proshkin et al. 2010; Dutta et al. 2011; Kohler et al. 2017; Saxena et al. 2018). This series of events can involve R-loops, which are RNA–DNA hybrids generated during transcription, by invasion of the DNA template strand by the nascent RNA (Thomas et al. 1976). R-loops are necessary for cell physiology but in excess can be harmful (Crossley et al. 2019), and their overabundance can be prevented by RNase HI function, which specifically degrades R-loops (Tadokoro and Kanaya 2009).

In this study, we show that DNA breaks caused by Rif^R and Str^R mutations are important contributors to their fitness cost. The involvement of R-loops in the generation of DNA breaks allowed us to identify RNase HI as an important modulator of the cost of resistance, which we validate using a repurposed drug. We further show that targeting RNase HI is a plausible strategy for the selective elimination of resistant bacteria, as lack of RNase HI leads to extinction of resistant clones when competing against sensitive bacteria in laboratory conditions, abolishing compensatory evolution. Importantly, eradication of resistant bacteria lacking RNase HI is remarkably efficient in the mammalian gut as well. Altogether, we reveal previously unknown factors that contribute to the fitness cost of antibiotic resistance and that can be exploited to selectively eliminate resistant bacteria in polymorphic populations.

Results

DNA Breaks Correlate with the Fitness Cost of Single- and Double-Resistant Clones

In order to test if Rif^R and Str^R mutations generate DNA breaks, and whether DNA breaks contribute to the cost of resistance, we simultaneously measured competitive fitness and activation of the SOS response, a well-established proxy specific for the occurrence of DNA breaks (Quillardet et al. 1982; Maslowska et al. 2019). We performed these assays in sensitive *Escherichia coli*, Str^R strains ($RpsL^{K43N}$, $RpsL^{K43T}$, and $RpsL^{K43R}$), Rif^R strains ($RpoB^{H526L}$, $RpoB^{H526Y}$, and $RpoB^{S531F}$), and double-resistant mutants carrying the nine possible combinations of these resistance alleles. Remarkably, 14 out of the 15 resistant strains show increased SOS activation (fig. 1A), demonstrating that resistance mutations, alone or in combination, cause DNA breaks. Moreover, the SOS induction is strongly correlated with the fitness cost of resistance (fig. 1B, $R^2 = 0.81$, $P = 2.4 \times 10^{-6}$). Among the set of mutants studied, costs and SOS induction are larger in double than in single-resistant mutants (fig. 1A), suggesting that the correlation may be driven by double mutants. However, single mutations known to generate large costs (Trindade et al. 2009) cause a strong induction of the SOS response (supplementary fig. S1, Supplementary Material online), and the correlation between cost and SOS induction is significant when only single mutants (those shown in fig. 1A and supplementary fig. S1, Supplementary Material online) are analyzed ($R^2 = 0.84$, $P = 4.7 \times 10^{-4}$). To independently confirm the occurrence of DNA breaks in resistant bacteria, we used a system which permits direct visualization of double-stranded DNA ends by live-cell fluorescence microscopy (Shee et al. 2013). We combined this system with the SOS reporter, and analyzed a subset of resistant mutants and sensitive bacteria. This corroborated that Rif^R and Str^R mutations indeed cause increased number of DNA breaks, also exhibiting the cell elongation phenotype typically caused by SOS-induced inhibitors of cell division (table 1 and supplementary fig. S2, Supplementary Material online). However, Rif^R and/or Str^R mutants do not show reduced cell viability (supplementary fig. S3A, Supplementary Material online), suggesting that the amounts of DNA breaks generated by these mutations lie within ranges manageable by bacterial mechanisms for prevention of cell death by genomic instability. In summary, these results demonstrate that Rif^R and Str^R mutations can cause DNA breaks, suggesting that DNA breaks are an additional contributor to their fitness cost.

Erythromycin-Resistant Clones Show Increased DNA Breaks

To understand if resistance mutations involving a different mechanism that can lead to perturbations of transcription–translation coupling would also generate DNA breaks, we studied erythromycin resistance mutations (Erm^R). Erythromycin targets the 50S ribosomal subunit, affecting translation and its coupling with transcription (Sedlyarova et al. 2017). Erm^R mutations, mapping to the genes *rplD* and *rplV* (encoding, respectively, the proteins L4 and L22 of the 50S ribosomal subunit), are known to reduce translation elongation rate (Chittum and Champney 1994; Zaman et al. 2007), likely affecting transcription–translation coupling. We isolated Erm^R clones carrying either $RplD^{G66R}$ or $RplV^{\Delta(82-84)}$ mutations and found that both mutants show fitness cost and increased SOS (fig. 1C), demonstrating that other resistance mutations, with different mechanistic basis but affecting the same process (transcription–translation coupling) also cause DNA breaks.

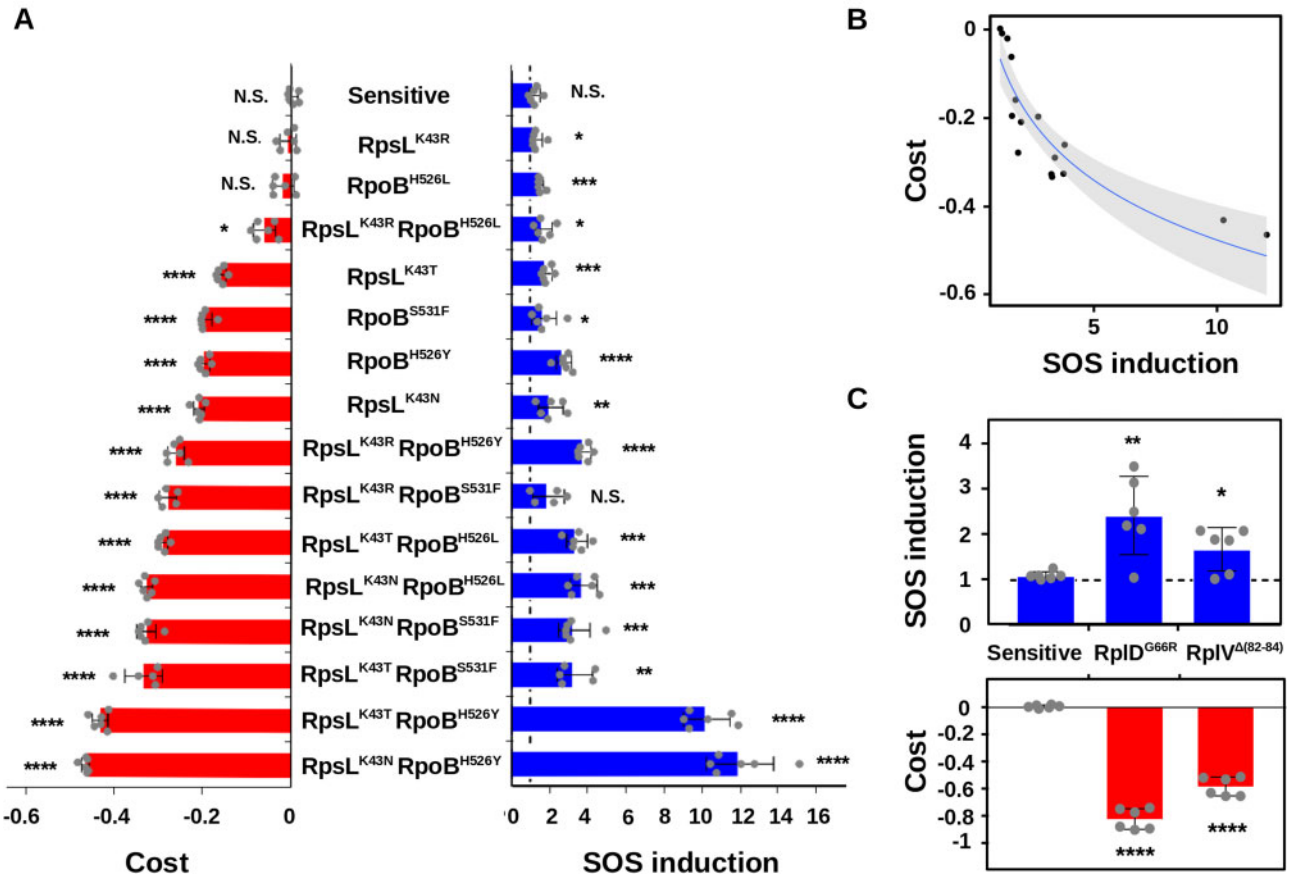

Fig. 1. DNA breaks correlate with the fitness cost of resistance. (*A*) Fitness cost (red bars) and SOS induction (blue bars) of sensitive bacteria and Str^R and Rif^R mutants in LB at 4 h. The strains are ordered from lower to higher fitness cost (top to bottom). The dashed line indicates no SOS induction. Error bars represent mean ± SD of independent biological replicates ($n \geq 5$). NS, nonsignificant; *$P < 0.05$; **$P < 0.01$; ***$P < 0.001$; ****$P < 0.0001$ (one-sample two-tailed Student's *t*-test). (*B*) Correlation between average fitness cost (*y* axis) and average SOS induction (*x* axis) per genotype, representing the data from (*A*). The blue line represents the logarithmic regression line, and the gray area represents the 95% CI. (*C*) SOS induction (blue bars) and fitness cost (red bars) of sensitive bacteria and Erm^R mutants in LB at 4 h. The dashed line indicates no SOS induction. Error bars represent mean ± SD of independent biological replicates ($n = 6$). NS, nonsignificant; *$P < 0.05$; **$P < 0.01$; ***$P < 0.001$; ****$P < 0.0001$ (one-sample two-tailed Student's *t*-test).

Table 1. Percentage of Cells Showing DNA Breaks (Gam-GFP Foci) in Sensitive and Resistant Bacteria Either in Wild-Type or Δ*rnhA* Backgrounds.

Δ*dam* (positive control)	**21.28%**
Sensitive	**0.72%**
***rpsL* (K43N)**	**0.73%**
***rpoB* (H526Y)**	**0.96%**
***rpsL* (K43N) *rpoB* (H526Y)**	**10.71%**
Δ*rnhA* (sensitive)	**9.27%**
Δ*rnhA rpsL* (K43N)	**33.92%**
Δ*rnhA rpoB* (H526Y)	**10.02%**
Δ*rnhA rpsL* (K43N) *rpoB* (H526Y)	**49.90%**

Note.—Except in the Δ*dam* positive control (in which over 100 cells sufficed to provide an illustrative example), at least 1,000 cells per group were analyzed (see also supplementary figs. S2 and S5, Supplementary Material online).

Compensatory Evolution Leads to a Reduction of DNA Breaks

We then reasoned that, if DNA breaks are contributing to the fitness cost of Rif^R and Str^R mutations, compensatory evolution of resistant strains should result in a reduction of DNA breaks. To test this, we compared the cost and SOS induction in the RpsL^{K43T} RpoB^{H526Y} double mutant and in an isogenic strain additionally carrying the most prevalent compensatory mutation found in our previous study: RpoC^{Q1126K} (Moura de Sousa et al. 2017). As hypothesized, both cost and SOS induction are greatly reduced in the compensated strain (fig. 2A), confirming that DNA breaks are targeted by compensatory evolution. To further test if DNA breaks are frequently reduced by compensatory evolution, we analyzed nine compensated clones from three independent populations of the RpsL^{K43T} RpoB^{H526Y} double mutant propagated for 15 days in the absence of antibiotics. As expected, the costs are smaller in the evolved strains and, as hypothesized, all the nine compensated clones show decreased SOS induction compared with their resistant ancestor (fig. 2B). This demonstrates that compensatory evolution repeatedly targets mechanisms that reduce DNA breaks, suggesting that DNA breaks are important contributors to the fitness cost of these antibiotic resistances.

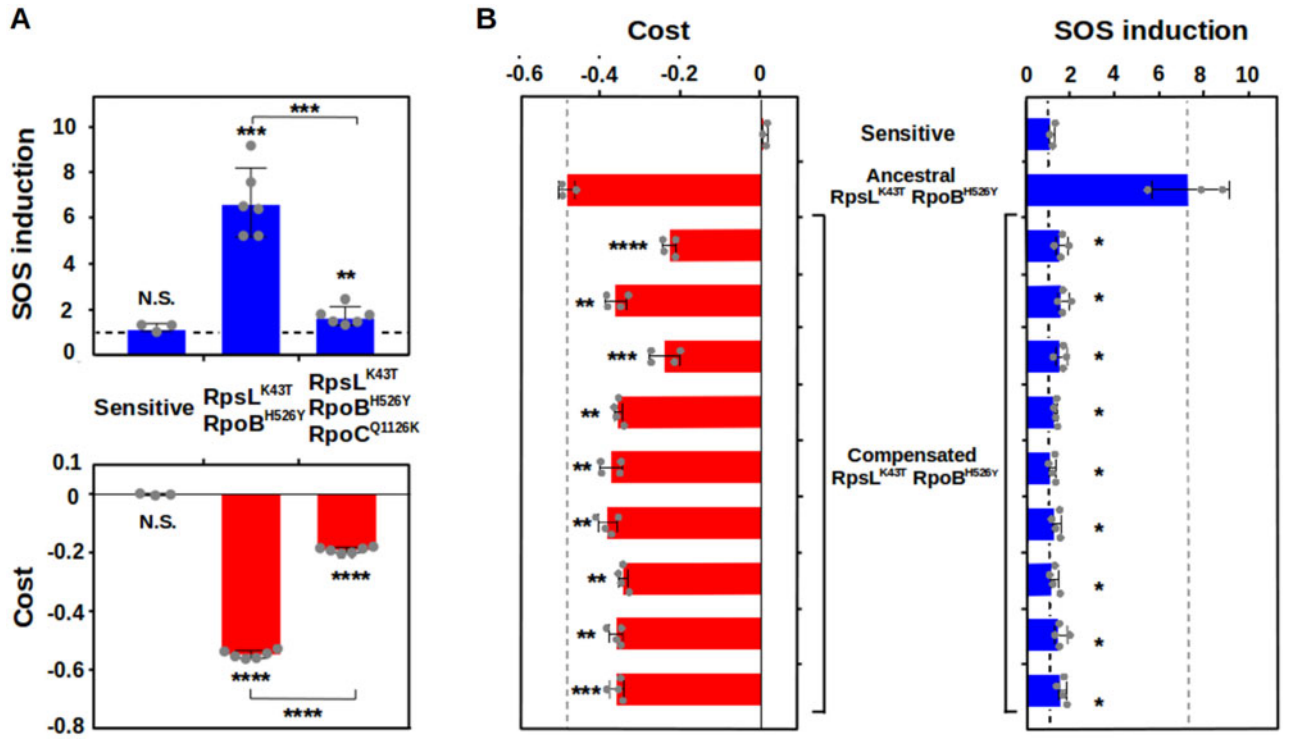

FIG. 2. Compensatory evolution cause reduction of DNA breaks. (*A*) SOS induction (blue bars) and fitness cost (red bars), of sensitive (left) double-resistant (center) and double-resistant carrying a compensatory mutation (right) bacteria in LB at 4 h. The dashed line indicates no SOS induction. Error bars represent mean ± SD of independent biological replicates ($n \geq 3$). NS, nonsignificant; *$P < 0.05$; **$P < 0.01$; ***$P < 0.001$; ****$P < 0.0001$ (one-sample two-tailed Student's *t*-test for evaluating individual genotypes, and two-tailed unpaired Student's *t*-test for comparing different genotypes). (*B*) Fitness cost (red bars), and SOS induction (blue bars) of sensitive, ancestral RpsL^{K43T} RpoB^{H526Y} and nine compensated clones in LB at 4 h. The black dashed line indicates no SOS induction. The gray dashed lines mark the cost/SOS of the ancestral double mutant. Error bars represent mean ± SD of independent biological replicates ($n \geq 3$). NS, nonsignificant; *$P < 0.05$; **$P < 0.01$; ***$P < 0.001$; ****$P < 0.0001$ (two-tailed unpaired Student's *t*-test).

Increasing Transcription-Coupled DNA Repair Reduces the Cost of Resistance

Given the results above, we hypothesized that the cost of Rif^R and Str^R mutations could be reduced by enhancing DNA repair. The RNA polymerase-binding transcription factor DksA has been recently shown to be involved in the transcription-coupled repair of DNA breaks (Myka and Gottesman 2019; Myka et al. 2019). Thus, we expect overexpression of *dksA* to decrease the cost of resistance. As hypothesized, overproduction of a plasmid-borne multicopy DksA increases the fitness of the double-resistant RpsL^{K43N} RpoB^{H526Y}, but not that of sensitive bacteria (supplementary fig. S4*A*, Supplementary Material online), indicating that the relationship between DNA breaks and the fitness cost of Rif^R and Str^R mutations is causal in this double mutant-resistant background.

Replication Speed Affects the Cost of Resistance

Transcription–translation uncoupling, which can be generated by rifampicin- or streptomycin-resistant alleles (Jensen 1988; Elgamal et al. 2016), can involve increased generation of replication–transcription conflicts, which ultimately generate DNA breaks (Dutta et al. 2011; Merrikh et al. 2012). Replication–transcription conflicts are maximized during fast replication, and less pronounced when bacteria grow slowly (Merrikh et al. 2011). Consequently, we hypothesized that the fitness cost of resistance mutations should be expressed mostly when cells are rapidly dividing. Indeed, we observed that, although the costs of Rif^R and Str^R mutations are similar at 4 and 24 h, these costs are generated in the first 4 h (which comprise exponential growth), whereas resistance mutations show no cost afterward, when growth slows down (fig. 3*A*). We therefore hypothesize that altering replication–transcription conflicts should affect the fitness cost of these resistance mutations. To test that hypothesis, we influenced the occurrence of replication–transcription conflicts through two strategies: negatively by growing our set of mutants in minimal medium, where DNA replication is slower (Wang and Koch 1978), or positively it by overproducing the DNA replication initiator protein DnaA, which causes simultaneous initiation of multiple replication forks (Skarstad et al. 1989). Our hypothesis predicts that DNA breaks should be reduced in minimal medium, where replication–transcription conflicts are expected to be less pronounced (fig. 3*B*). In agreement with our hypothesis, the SOS induction is smaller in minimal than in rich media (fig. 3*C*, right panel), and a weaker correlation with the cost is found in minimal medium (supplementary fig. S4*B*, Supplementary Material online, $R^2 = 0.28$, $P = 0.034$). Coherently, the number of resistant mutants showing a fitness cost is smaller in minimal medium

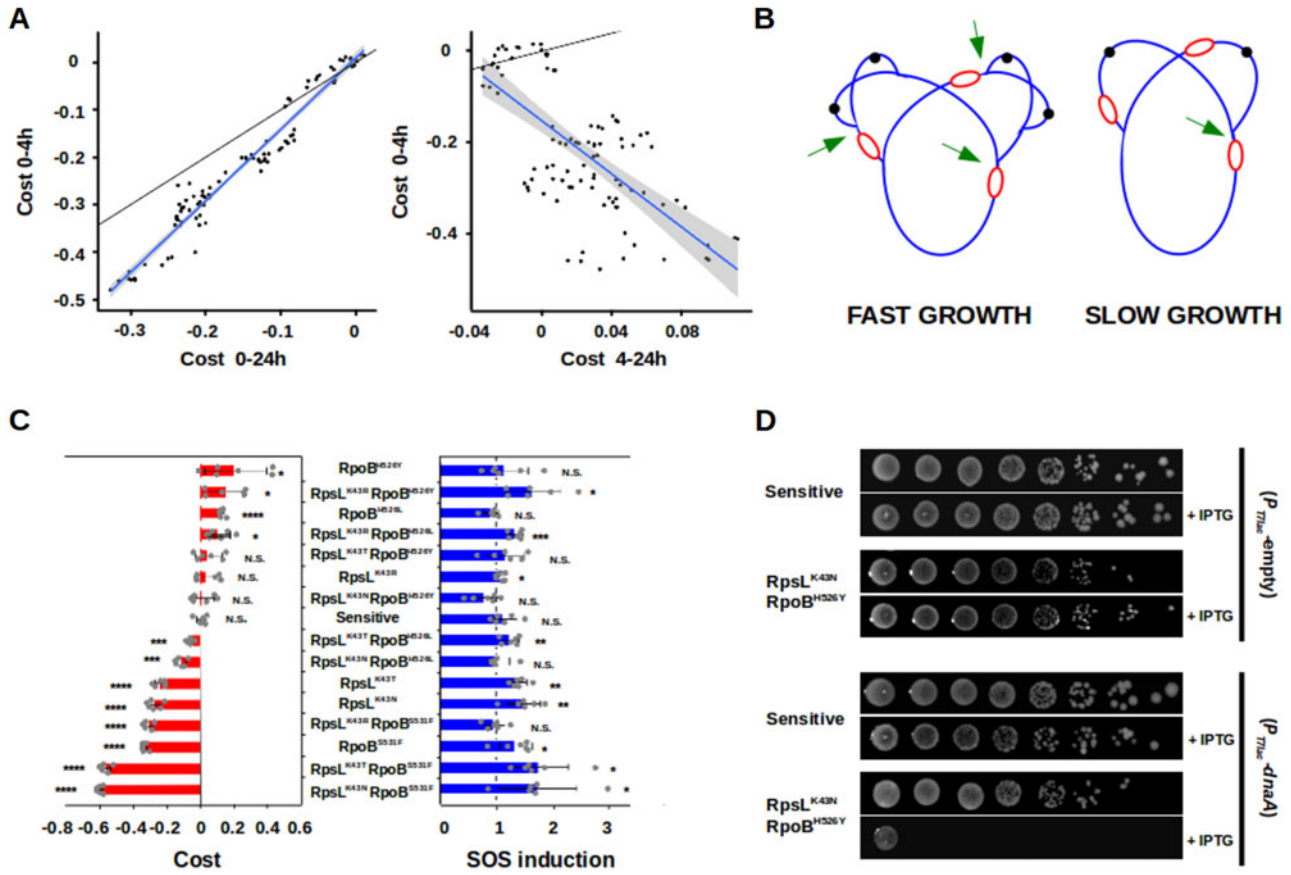

FIG. 3. Replication speed affects the cost of resistance. (*A*) Left panel: correlation of the fitness cost between time 0 and 4 h (*y* axis) and between time 0 and 24 h (*y* axis), in LB. Right panel: correlation of the fitness cost between time 0 and 4 h (*y* axis) and between time 4 and 24 h (*y* axis), in LB. Black lines represent the linear regressions if the costs were identical. Blue lines represent the regression lines, and the gray areas represent the 95% CIs. Data from the experiments shown in figure 1*A*. (*B*) Schematic representation of DNA replication of *Escherichia coli* during fast (left) or slow (right) growth. Black dots represent the origin of replication, and red lines represent transcription forks; green arrows mark regions of potential replication–transcription conflicts. (*C*) Fitness cost (red bars), and SOS induction (blue bars) of sensitive bacteria and Str^R and/or Rif^R mutants in minimal medium at 8 h. The strains are ordered from lower to higher cost (top to bottom). The dashed line indicates no SOS induction. Error bars represent mean ± SD of independent biological replicates ($n = 6$). NS, nonsignificant; $^*P < 0.05$; $^{**}P < 0.01$; $^{***}P < 0.001$; $^{****}P < 0.0001$ (one-sample two-tailed Student's *t*-test). (*D*) Aliquots of serial dilutions (approximately from 5×10^7 to 5 cells) of sensitive and $RpsL^{K43N}$ $RpoB^{H526Y}$ strains carrying the expression vector pCA24N -gfp, either empty (top, strains RB1317 and RB1321) or harboring the gene *dnaA* (bottom, strains RB1290 and RB1294) and either in the absence or the presence of the inducer IPTG. Each experiment included three biological replicates and three experiments were performed; representative data sets are shown.

(8, compared with 13 in rich medium), with four of them even showing a higher fitness than sensitive bacteria (fig. 3*C*, left panel). Moreover, mutations that are costly and show strong SOS induction in rich medium (e. g. $RpsL^{K43N}$ $RpoB^{H526Y}$ and $RpsL^{K43T}$ $RpoB^{H526Y}$) generate much smaller costs and SOS induction in minimal medium (compare fig. 1*A* with fig. 3*C*). Besides this general trend, however, there are resistant mutants (notably, those carrying the allele $RpoB^{S531F}$) that conserve or even increase their fitness cost in minimal medium (compare fig. 1*A* with fig. 3*C*), evidencing the coexistence of diverse factors contributing to the cost of resistance (such as the extensively described defects in protein synthesis). Conversely, our hypothesis also anticipates that increasing the occurrence of replication–transcription conflicts by overproducing DnaA should particularly affect resistant bacteria. As hypothesized, overexpression of *dnaA* severely compromises the viability of double-resistant bacteria, whereas sensitive bacteria remain largely unaffected (fig. 3*D*). Altogether, these results demonstrate the involvement of replication–transcription conflicts in the generation of the cost of Rif^R and Str^R mutations, also corroborating the important contribution of DNA breaks to it.

RNAse HI Strongly Influences the Fitness of Resistant Bacteria

Both transcription–translation uncoupling and replication–transcription conflicts lead to increased formation of R-loops, which cause DNA breaks (Dutta et al. 2011; Lang et al. 2017) and boost replication–transcription conflicts themselves by impairing replication fork progression (Gan et al. 2011). We thus reasoned that depleting RNase HI function, which specifically degrades R-loops (Tadokoro and Kanaya 2009), should lead to increased DNA breaks and fitness costs of

Rif^R and Str^R mutations. Accordingly, both DNA breaks and the cost of resistance are greatly increased in the Δ*rnhA* background (fig. 4*A*, table 1, and supplementary figs. S5 and S6*A*, Supplementary Material online), and cell viability is severely compromised in most resistant genotypes (supplementary fig. S3*B*, Supplementary Material online). Conversely, mild overproduction of RNase HI can ameliorate both DNA breaks and cost in a subset of mutants (supplementary fig. S7, Supplementary Material online); however, strong overproduction is toxic for the cell (Stockum et al. 2012; Wimberly et al. 2013), irrespective of its genotype (supplementary fig. S8, Supplementary Material online). These results suggest that R-loops are involved in the production of DNA breaks caused by Rif^R and/or Str^R mutations and that RNase HI can be a target for specifically manipulating the fitness of resistant strains in bacterial populations.

RNase HI Can Serve as a Target Specific against Resistant Bacteria

The large effect of lacking RNAse HI function on the fitness of resistant bacteria prompted us to ask whether targeting this protein could be used to select specifically against resistant bacteria in polymorphic populations. RNase HI inhibitors are currently studied as antiretrovirals (Tramontano et al. 2019). A commercially available one, RHI001, inhibits the activity of purified *E. coli* RNase HI protein in vitro*in vitro* (Kim et al. 2013). We observed that adding RHI001 to competitions between sensitive and resistant bacteria increases the fitness cost of resistant mutants (fig. 4*B*), on average by 14%, not affecting sensitive bacteria, either in a wild-type or in a Δ*rnhA* background (supplementary fig. S9, Supplementary Material online). RHI001 also reduces fitness of double-resistant bacteria more than that of sensitive bacteria during individual growth, in the absence of competition (supplementary fig. S6*B* and *C*, Supplementary Material online). Chemical inhibition is less effective than genetic removal (which increases cost on average by 28%) (fig. 4*C* and *D*), as may be expected, since stability, diffusibility across the bacterial envelope, pharmacokinetics, and pharmacodynamics of RHI001 in vivo are unknown, and potentially suboptimal. Nevertheless, these results suggest that inhibiting RNase HI may be a plausible strategy to select specifically against resistant strains coexisting with sensitive bacteria, as long as resistant strains fail to evolve adaptations that abrogate their extinction. In order to test this hypothesis, we propagated a mixture of sensitive bacteria (CFP-labeled) competing against a pool of five single-resistant mutants (YFP-labeled $RpsL^{K43N}$, $RpsL^{K43T}$, $RpoB^{H526L}$, $RpoB^{H526Y}$, and $RpoB^{S531F}$) during 15 days, in the absence of antibiotics. We followed the frequency dynamics of resistant clones under both strong bottlenecks (1:1,500 dilutions), where new adaptive mutations are less likely to spread, and weak bottlenecks (1:50 dilutions), where propagation of adapted clones is more probable. In parallel, we performed identical propagations, but in which all strains lack RNase HI, as a proxy for optimal inhibition of RNase HI function. We observed that, in the presence of RNase HI, sensitive bacteria initially outcompete resistant clones but, as the propagation progresses, resistant bacteria increase in frequency—likely due to the acquisition of compensatory and/or adaptive mutations—finally reaching coexistence (fig. 5*A*, blue lines). Remarkably, in the propagations of strains lacking RNase HI, resistant bacteria were completely outcompeted and went extinct by day 7 (fig. 5*A*, red lines) even under mild bottlenecks (fig. 5*B*).

Loss of RNase HI Function Selects against Resistant Bacteria in the Mammalian Gut

Since the outcome of competitions under laboratory conditions can differ from those within the host (Melnyk et al. 2015; Vogwill and MacLean 2015), we next tested if inhibition of RNase HI would be an effective strategy in an animal model. We used the well-established mouse gut colonization model, which resembles the natural environment of many bacterial pathogens, including *E. coli* (Sousa et al. 2017). We colonized by oral gavage two cohorts of mice (each $n = 6$): one with a 1:9 ratio mixture of CFP-tagged sensitive bacteria and a YFP-labeled double-resistant strain ($RpsL^{K43T}$ $RpoB^{H526Y}$, selected based on its ability to efficiently colonize the mammalian gut exhibiting low fitness cost; Leónidas Cardoso et al. 2020), and the other with an identical mixture but in which both strains are Δ*rnhA*. We then followed the frequency and absolute numbers (colony forming units [CFUs] per gram of feces) of the resistant strains over time. We found that, when RNase HI function is intact, the double-resistant strain persists in the gut of all animals at frequencies between 2.3% and 9.3% (fig. 5*C*, blue lines) and high bacterial loads (fig. 5*D*, blue lines) two weeks after gavage. Remarkably, in the absence of RNase HI, resistant clones are rapidly outcompeted by sensitive bacteria (fig. 5*C* and *D*, red lines). Indeed, resistant bacteria are driven to extremely low frequencies in as soon as 1-day postcolonization, and their extinction occurs in all the six mice in 5 days (fig. 5*C* and *D*, red lines), demonstrating that RNase HI is a novel target for efficiently and specifically eliminating resistant strains in the mammalian gut. Surprisingly, the absence of RNase HI does not lead to any detectable fitness defect in the sensitive bacteria, as the loads of *E. coli* are similar in the two cohorts of mice (fig. 5*E*). We then queried if the sequential application of an antibiotic treatment upon competition between sensitive and resistant genotypes under conditions of RNase HI depletion could successfully eliminate the entire bacterial population. In this scenario, we hypothesize that an antibiotic treatment should render completely different outcomes depending on the presence of RNase HI function. Indeed, a week-long treatment of streptomycin starting at day 16 after gavage enables resistant clones with intact RNase HI function to rebound and reach high loads (10^7–10^8 CFUs/g feces), but it completely eradicates Δ*rnhA* bacteria in all the six mice (fig. 5*F*). These results demonstrate that RNAse HI function is not only a key determinant of the fitness of resistant bacteria, but also a potential target for coadjuvant drugs to eliminate undesirable bacteria in a natural environment for bacterial pathogens such as the mammalian gut. Altogether, these results show the potential of targeting RNase HI as a promising resistance-specific antimicrobial therapy.

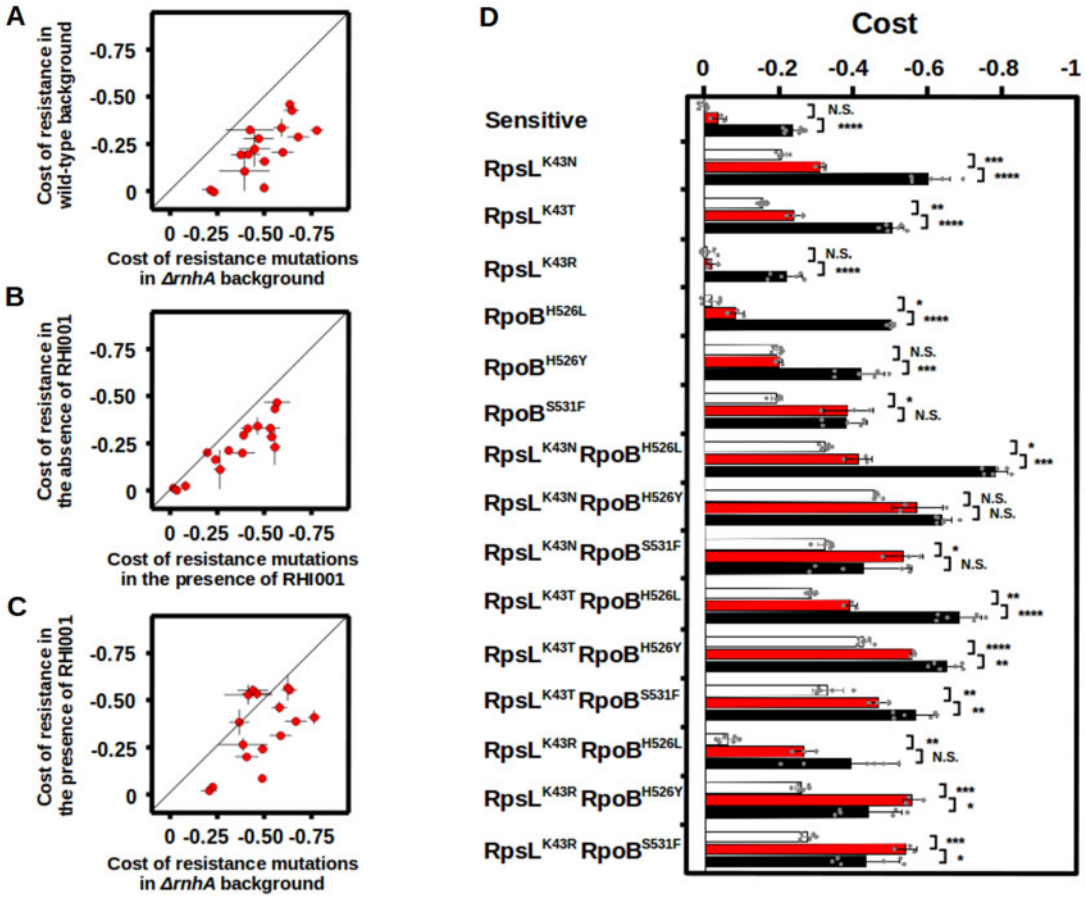

FIG. 4. RNAse HI strongly influences the fitness of resistant bacteria. (*A*) Correlation between the fitness cost of resistance mutations in wild-type (*y* axis) or Δ*rnhA* backgrounds (*x* axis). The values corresponding to the wild-type background (*y* axis) are those already shown in figure 1A. The values corresponding to the Δ*rnhA* background (*x* axis) are those shown in supplementary figure S6A, Supplementary Material online. (*B*) Correlation between the fitness cost of resistance mutations in the absence of the RNase HI inhibitor (*y* axis) or in its presence (*x* axis). The values corresponding to the absence of the RNase HI inhibitor (*y* axis) are those already shown in figure 1A. (*C*) Correlation between the fitness cost of resistance mutations in the presence of the RHI001 (*y* axis) or in the Δ*rnhA* background (*x* axis). The values corresponding to the Δ*rnhA* background (*x* axis) and to the presence of RHI001 (*y* axis) are those already shown in panels (*A*) and (*B*), respectively. Error bars represent mean ± SD of independent biological replicates ($n \geq 3$). The black line in panels (*A*–*C*) represents the linear regression if the costs were identical. (*D*) Fitness cost of sensitive bacteria and Str^R and/or Rif^R mutants in the presence of the RNase HI inhibitor RHI001 (red bars). For comparison, the corresponding values in the absence of the inhibitor (data from the experiments shown in fig. 1A) or in a Δ*rnhA* background (data from the experiments shown in panel *A* and supplementary fig. S6A, Supplementary Material online) are represented as white and black bars, respectively. Error bars represent mean ± SD of independent biological replicates ($n = 3$). NS, nonsignificant; $^*P < 0.05$; $^{**}P < 0.01$; $^{***}P < 0.001$; $^{****}P < 0.0001$ (two-tailed unpaired Student's *t*-test) (see also supplementary figs. S6–S8, Supplementary Material online).

Discussion

The fitness costs of Rif^R and Str^R mutations are typically associated with altered protein synthesis (Andersson and Levin 1999; Andersson and Hughes 2010; Melnyk et al. 2015; Vogwill and MacLean 2015; Durão et al. 2018). However, certain mutations (e.g., $RpsL^{K43N}$ $RpoB^{H526Y}$ and $RpoB^{R529H}$) that cause limited alterations in biosynthesis (Zhou et al. 2013; supplementary fig. S10, Supplementary Material online) with respect to sensitive bacteria or to resistant strains with unaffected protein synthesis (e.g., $RpsL^{K43R}$; Neidhardt et al. 1996) can generate large costs (Trindade et al. 2009, fig. 1A and supplementary fig. S1, Supplementary Material online). Here we show that antibiotic resistance mutations affecting transcription and translation generate DNA breaks, which strongly correlate with their fitness cost (fig. 1, table 1, and supplementary figs. S1 and S2, Supplementary Material online). This suggests that multiple factors contribute to the fitness cost of resistance mutations affecting transcription and/or translation, namely deficient protein synthesis, altered transcriptome, and DNA breaks. In that scenario, the relative contribution of each factor to the fitness cost of resistance depends on the allele(s) and epistatic interactions involved, and on the conditions of the environment where the resistant clones strive.

Compensatory evolution of resistant bacteria (Moura de Sousa et al. 2017) suggested that Rif^R and Str^R resistance mutations can cause uncoupling between transcription and translation, which can result in DNA breaks (Dutta et al. 2011). Indeed, mutations conferring resistance to rifampicin or streptomycin have been previously shown to affect the coordination between transcription and translation (Jensen 1988; Elgamal et al. 2016). Agreeingly, we observed that the

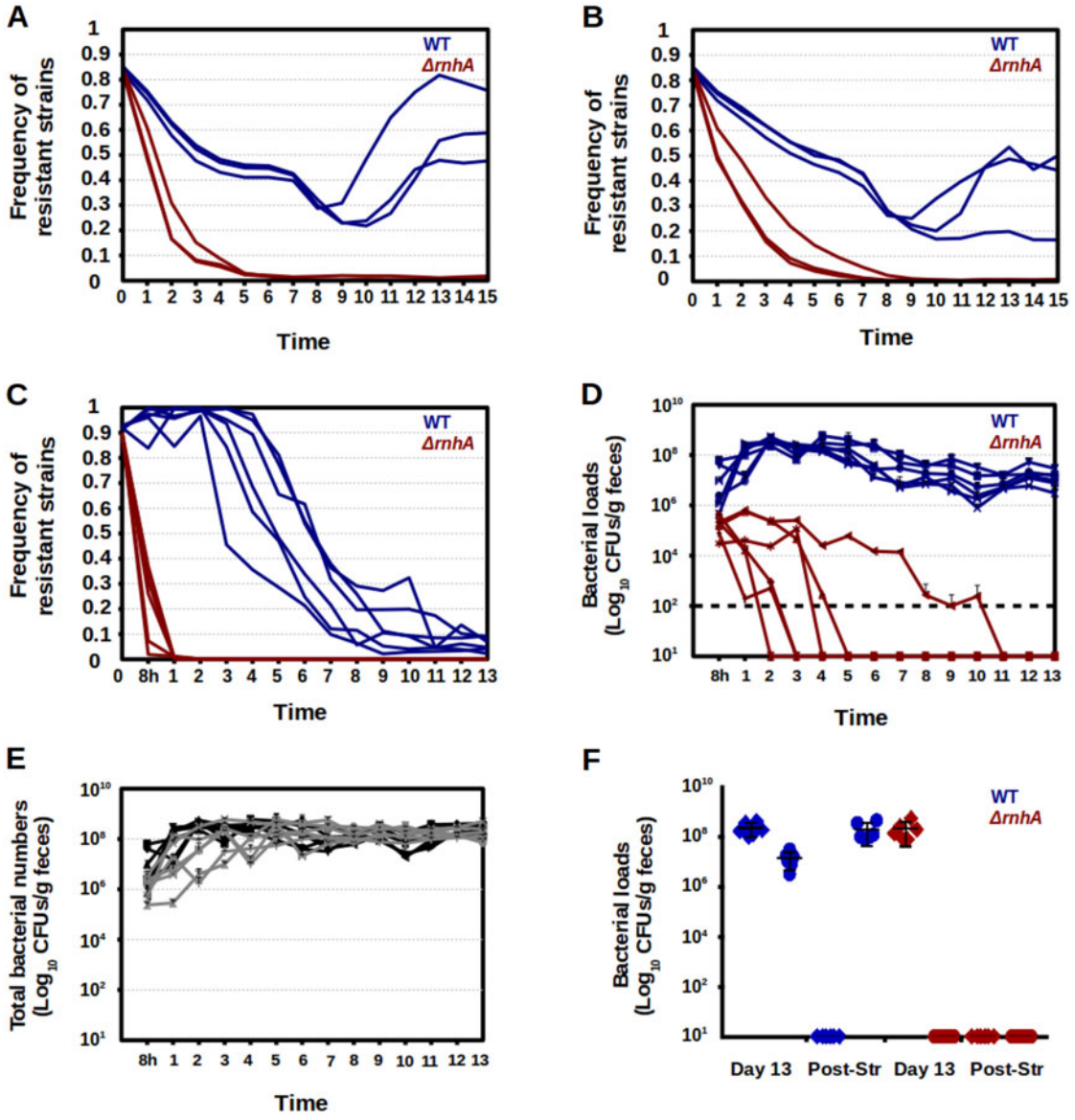

FIG. 5. Lack of RNase HI favors outcompetition of resistant mutants by sensitive bacteria. (*A* and *B*) Frequency of single-resistant mutants during three independent long-term competitions in rich medium against sensitive bacteria either in a genetic background including RNase HI (blue lines) or in a Δ*rnhA* background (red lines), imposing a strong (1:1,500 dilutions, *A*) or a mild (1:50 dilutions, *B*) bottlenecks. (*C* and *D*) Frequency (*C*) and bacterial loads ($\log_{10}$ CFUs/g feces, *D*) of double-resistant mutants during six independent long-term competitions against sensitive bacteria in mice, either in genetic backgrounds including RNase HI (blue lines) or in Δ*rnhA* backgrounds (red lines). Data are represented until extinction was observed in all six animals (13 days in the competitions in Δ*rnhA* backgrounds). The black dashed line represents the limit of detection. (*E*) Total (sensitive + double mutant) bacterial loads ($\log_{10}$ CFUs/g feces) of the strains carrying RNase HI (black lines) or in the Δ*rnhA* background (gray lines) during the competitions in the mouse gut. (*F*) Bacterial loads ($\log_{10}$ CFUs/g feces) at day 13 after gavage and after the week-long streptomycin treatment of sensitive (diamonds) and double-resistant bacteria (circles) either in a genetic background carrying RNase HI (blue) or in a Δ*rnhA* background (red). Error bars represent mean ± SD of the results in different mice ($n = 6$).

$RpsL^{K43N}$ $RpoB^{H526Y}$ and $RpsL^{K43T}$ $RpoB^{H526Y}$ double mutants, which combine alleles that cause increased transcription elongation rate (Fisher and Yanofsky 1983) and decreased translation rate (Schrag and Perrot 1996; Hosaka et al. 2004), show high costs and DNA breaks (fig. 1*A*). Curiously, inhibition of translation has been shown to alleviate the cost of Rif^R mutations in *Pseudomonas aeruginosa* (Hall et al. 2011). This observation is compatible with a scenario in which, as Rif^R mutations cause a perturbation of transcription–translation coupling by virtue of reduced RNA polymerase processivity, translation inhibitors promote recoupling by decreasing ribosomal activity. If correct, this suggests that, in certain cases, the benefit of regaining transcription–translation coupling could surpass the cost of undergoing reduced protein synthesis. We also showed that RNase HI is a key modulator of the fitness of resistant mutants (fig. 4, table 1, and supplementary figs. S5, S6A, S7, and S8, Supplementary Material online). Interestingly, transcription–translation uncoupling caused by chemical inhibition of translation can generate R-loops (Broccoli et al. 2004; Dutta

et al. 2011; Negro et al. 2019). Thus, perturbations of the coupling between transcription and translation increase the requirement of RNase HI function by bacteria. This opens the possibility to designing novel therapeutic interventions by combining drugs targeting transcription or translation with RNase HI inhibitors in order to enhance the effectiveness of antimicrobial treatments.

We observed that replication–transcription conflicts contribute to the fitness cost of Rif^R and Str^R mutations (fig. 3), and that overproduction of DksA, involved in transcription-coupled DNA repair (Myka and Gottesman 2019; Myka et al. 2019), reduces the cost of resistance (supplementary fig. S4*A*, Supplementary Material online). Interestingly, DksA is also involved in preventing replication–transcription conflicts (Tehranchi et al. 2010). Thus, prevention of these conflicts by DksA might also account for its beneficial effect on resistant bacteria, besides the enhancement of DNA repair. The involvement of replication–transcription conflicts in the cost of resistance is coherent with previous observations, such as the small cost of specific Rif^R and/or Str^R alleles in minimal medium (Paulander et al. 2009; Trindade et al. 2012; Durão et al. 2015) or the outcompetition of sensitive bacteria by resistant mutants in aging colonies (Wrande et al. 2008; Katz and Hershberg 2013). Interestingly, stable DNA replication (initiation of DNA replication at sites different from *OriC*) can be induced by lack of RNase HI or by conditions that activate SOS (Kogoma 1997). Thus, Rif^R and Str^R mutations, which induce SOS (fig. 1 and supplementary figs. S1 and S2, Supplementary Material online), could additionally favor replication–transcription conflicts via induction of stable DNA replication. This can generate a feed-forward loop of synergistic deleterious effects, which may be further enhanced by the fact that induction of the SOS response causes down-regulation of *rnhA* (Quiñones et al. 1987). This detrimental runaway loop, as well as the effects of the environment on the fitness cost described above (figs. 1*A* and 3*C*), could potentially be exploited therapeutically, via concurrent chemical and dietary interventions designed to synergistically maximize the cost of resistance.

We revealed RNase HI as a promising target specific against resistant bacteria (fig. 4), and showed that lack of RNase HI function favors extinction of resistant clones in polymorphic populations, preventing compensatory evolution (fig. 5*A* and *B*). Importantly, we demonstrated that loss of RNase HI leads to the efficient elimination of resistant clones competing against sensitive bacteria in an animal model as well (fig. 5*C* and *D*). Interestingly, sensitive bacteria lacking RNase HI do not show fitness defects in the gut (fig. 5*E*), which hampers the development of resistance to RNase HI inhibition. Moreover, targeting RNase HI prevents recurrence of resistant bacteria upon an antibiotic treatment, favoring the elimination of the entire bacterial population (fig. 5*F*). These notions are specially important for resistances mediated by mutations (Hershberg 2017) or for pathogens that acquire antibiotic resistance exclusively through mutation, such as *Mycobacterium tuberculosis*, which often carries Rif^R and Str^R mutations (Almeida Da Silva and Palomino 2011). Interestingly, RNase HI has been proposed as an antimycobacterial target due to its essentiality in *Mycobacterium smegmatis* (Minias et al. 2015; Gupta et al. 2017). The results presented here strongly support the plausibility of this strategy. However, in the case of mycobacteria, the essentiality of the RNase HI function might facilitate the development of resistance against drugs targeting it. Also, the slow growth of certain mycobacteria, such as *M. tuberculosis*, might significantly affect the phenomena described here, potentially altering the efficacy of RNase HI targeting as antimycobacterial strategy.

An understanding of the determinants of maintenance and dissemination of antibiotic resistance, such as its fitness cost, is urgently needed (World Health Organization 2018). We show that DNA breaks are important contributors to the fitness cost of resistance mutations affecting transcription and translation and reveal RNase HI as a promising antimicrobial target specific against resistant bacteria, which we validated under laboratory conditions, in the mammalian gut, and by using a repurposed drug. Overall, our results uncover important effects of resistance mutations on bacterial physiology and evolution, and demonstrate the plausibility of exploiting these effects to develop novel strategies against antibiotic-resistant bacteria, in line with the recently proposed eco-evo approaches to tackle the global challenge of antibiotic resistance (Baquero et al. 2011; Andersson et al. 2020).

Materials and Methods

Bacterial Strains, Media, and Growth Conditions

All the strains used in this study (supplementary data S1, Supplementary Material online) derive from strains RB266, RB323, or RB324, which are derivatives of *E. coli* K12 MG1655 (Blattner et al. 1997). Fluorescently labeled strains harbor a copy of either yellow fluorescent protein (YFP) or cyan fluorescent protein (CFP) under the control of the LacI-regulated promoter P_{LacO-1} inserted either in the *yzgL* pseudogene locus or in the *galK* gene, a deletion comprising the entire *lac* operon (to make constitutive the expression of the fluorescent proteins), and the SOS reporter construction P_{sulA}-*mCherry* inserted in the *ysaCD* pseudogene locus. The SOS reporter fusion was constructed by replacing a *tetA-sacB* selectable/counterselectable marker (Li et al. 2013) located upstream from a *mCherry-FRT-aph-FRT* cassette, previously inserted in the *ysaCD* locus, by the regulatory regions (150 bp upstream from the translation initiation site) of the SOS-regulated gene *sulA*. Resistant mutants additionally carry different chromosomal alleles conferring antibiotic resistance. The fluorescent constructions were generated by Lambda-Red recombineering (Datsenko and Wanner 2000; Murphy et al. 2000; Yu et al. 2000), followed by transference to a clean background by P1 transduction (Lennox 1955), and subsequent transduction of the resistance alleles. The clean deletion of *rnhA* was constructed by markerless recombineering using a *tetR-*P_{tet}*-ccdB-cat* selection/counterselection cassette as described by Figueroa-Bossi and Bossi (2015), and subsequent transfer of the markerless deletion to a clean background by P1 transduction, using as recipient an isogenic

strain carrying a deletion of the nearby gene *proB*, which causes proline auxotrophy, and selecting for growth in minimal medium. The presence of each construction/mutation was assessed by PCR-mediated amplification of the corresponding region and Sanger sequencing. The Gam-GFP construction (Shee et al. 2013) was generously contributed by Professor Susan M. Rosenberg. The chromosomal construction comprising a copy of the *rnhA* gene under the control of a promoter inducible by arabinose (Stockum et al. 2012) was kindly donated by Dr. Christian J. Rudolph. Derivatives of these strains carrying the P_{sulA}-*mCherry* and different resistance mutations were constructed by P1 transduction. The plasmid pRB-5 (carrying the *rnhA* gene under the control of a promoter inducible by anhydrotetracycline) was constructed by PCR amplification of the vector pZS*11 (Subramaniam et al. 2013) and the construction *tetR*-$P_{LTetO-1}$-*rnhA* from strain RB1207, subsequent restriction with AatII and HindIII enzymes, ligation, and electroporation. The construction *tetR*-$P_{LTetO-1}$-*rnhA* in strain RB1207 was made by Lambda-Red recombineering (Datsenko and Wanner 2000; Murphy et al. 2000; Yu et al. 2000), and selection/counterselection (Li et al. 2013), over a previous $P_{LtetO-1}$-*sfGFP* construction (Balbontín et al. 2014). The plasmids carrying an inducible copy of either *dksA* or *dnaA* were obtained from the ASKA library of *E. coli* ORF clones (Kitagawa et al. 2005). Cultures were grown in either lysogeny broth (LB, Miller formulation) (Bertani 1951) or M9 broth supplemented with 0.4% glucose (Sambrook et al. 1989), in round-bottom 96-well plates incubated at 37 °C with shaking (700 rpm) in a Grant-bio PHMP-4 benchtop incubator, unless indicated otherwise. Solid medium was LB containing 1.5% agar. Media were supplemented when necessary with antibiotics at the following concentrations: rifampicin (100 μg/ml), streptomycin (100 μg/ml), ampicillin (100 μg/ml), erythromycin (150 μg/ml), kanamycin (100 μg/ml), and chloramphenicol (25 μg/ml).

Competitive Fitness/SOS Induction Assays

The relative fitness (selection coefficient per generation) of each YFP-tagged-resistant strain carrying the SOS reporter was measured by competitive growth against a CFP-labeled isogenic sensitive strain *E. coli* K12 MG1655 also carrying the SOS reporter. The formula used to calculate the selection coefficient was $s = [\ln(NRf/NSf) - \ln(NRi/NSi)]/\ln(NSf/NSi)$, being ***NRi*** and ***NRf*** the initial and final number of resistant bacteria, and ***NSi*** and ***NSf*** the initial and final number of sensitive bacteria. The competitor strains were first streaked out of their respective frozen vials, then individual colonies were inoculated separately in medium without antibiotics and incubated overnight (approximately 16 h); the next morning, the number of cells in each culture was measured by Flow Cytometry, and 10 μl of 1:1 mixtures of YFP and CFP bacteria were added to 140 μl of medium, at an initial number of approximately 10^6 cells. The initial and final frequencies of the strains were obtained by counting their cell numbers in the Flow Cytometer. The number of generations was estimated from that of the reference sensitive strain (approximately five generations at 4 h, and approximately eight generations at 24 h), and the selection coefficient was determined as described above for each independent competition. The proportion of SOS-induced bacteria was quantified as the number of either YFP-tagged or CFP-labeled bacteria showing red fluorescence (from the P_{sulA}-*mCherry* SOS reporter fusion) above a threshold determined by the fluorescence levels of the control strains *lexA (ind-)* (constitutive repression of the SOS response) and Δ*lexA* (constitutive activation of the SOS response) (Lin and Little 1988). The data represented are the induction level of each resistant mutant normalized with respect to the induction levels of the sensitive it is competing against. In the competitions including the RNase HI inhibitor 2-[[[3-Bromo-5-(2-furanyl)-7-(trifluoromethyl)pyrazolo[1,5-a]pyrimidin-2-yl]carbonyl]amino]-4,5,6,7-tetrahydro-benzo[b]thiophene-3-carboxylic acid ethyl ester (RHI001, Glixx Laboratories Inc., catalog number GLXC-03982), the medium was supplemented with 500 μM of RHI001.

Flow Cytometry

A BD LSR Fortessa SORP flow cytometer was used to quantify bacteria, using a 96-well plate High-Throughput Sampler (HTS) and SPHERO fluorescent spheres (AccuCount 2.0 μm blank particles), in order to accurately measure volumes. Bacterial numbers were calculated based on the counts of fluorescently labeled bacteria with respect to the known number of beads added to a given volume. The instrument was equipped with a 488-nm laser used for scatter parameters and YFP detection, a 442-nm laser for CFP detection, and a 561-nm laser for mCherry detection. Relative to optical configuration, CFP, GFP, YPF, and mCherry were measured using bandpass filters in the range of 470/20, 530/30, 540/30, and 630/75 nm, respectively. The analyzer is also equipped with a forward scatter (FSC) detector in a photomultiplier tube (PMT) to detect bacteria. The samples were acquired using FACSDiVa (version 6.2) software, and analyzed using FlowJo (version 10.0.7r2). All Flow Cytometry experiments were performed at the Flow Cytometry Facility of the Instituto Gulbenkian de Ciência (IGC), Oeiras, Portugal.

Selection for Erm^R Bacteria

Fifteen independent colonies of sensitive bacteria were separately inoculated in LB in a 96-well plate, incubated at 37 °C with shaking (700 rpm) for 7 h, and 0.1 ml of either independent culture was plated onto a LB agar plate supplemented with 150 μg/ml erythromycin, and incubated at 37 °C for 5 days (Erm^R strains grow in the presence of erythromycin, albeit slowly). Colonies able to grow in these plates were streaked onto plates supplemented with 150 μg/ml erythromycin, in order to further assess their bona fide resistance, and the *rplD*, and *rplV* genes of the resistant clones were amplified by PCR and analyzed by Sanger sequencing.

Microscopy

Early exponential cultures were diluted into prewarmed medium containing the inducer of the Gam-GFP construction (anhydrotetracycline, 25 ng/ml) and incubated at 37 °C with shaking (240 rpm) for 3 h, prior to imaging. Bacterial solutions were then placed onto 1% agarose (in 1× PBS) pads mounted

in adhesive frames between the microscope slide and a coverglass. Images were acquired on an Applied Precision DeltavisionCORE system, mounted on an Olympus IX71 inverted microscope, coupled to a Cascade II 1,024 × 1,024 EM-CCD camera, using an Olympus 100× 1.4 NA Uplan SAPO Oil immersion objective, where GFP and mCherry were imaged with FITC (Ex: 475/28, EM: 528/38) and TRITC (Ex: 542/28, Em: 617/73) fluorescence filter sets, respectively, and DIC optics. Images were deconvoluted with Applied Precision's softWorx software, and prepared for presentation (cropping smaller fields to facilitate visualization, and false-coloring green and red fluorescent signals) using Fiji/ImageJ. All microscopy experiments were performed at the Imaging Facility of the IGC.

Spot Assays

For viability assays, sensitive and resistant strains were first streaked out of their respective frozen vials, then individual colonies were inoculated separately in medium without antibiotics and incubated overnight (approximately 16 h); the next morning, the number of cells in each culture was measured by Flow Cytometry, and bacteria were appropriately diluted in 1× PBS to generate solutions containing approximately 10^8, 10^7, 10^6, 10^5, 10^4, or 10^3 cells/ml. Then 5 µl aliquots of these bacterial solutions (approximately 5×10^5 to 5 cells) were spotted onto LB agar plates and incubated overnight at 37 °C. For *dnaA* overexpression experiments, sensitive and RpsL^{K43N} RpoB^{H526Y} strains carrying the expression vector pCA24N -gfp, either empty or carrying the *dnaA* gene (Kitagawa et al. 2005) were streaked individually onto LB agar plates supplemented with the appropriate antibiotic (to select for the presence of the plasmid), and incubated overnight at 37 °C. The next day, three independent colonies from each strain were inoculated separately in LB supplemented with the appropriate antibiotic (150 µl per well) in a 96-well plate and incubated overnight at 37 °C with shaking (700 rpm). The next day, the OD_{600} of the overnight cultures was measured using a Thermo Scientific Multiskan Go spectrophotometer, bacteria were appropriately diluted in 1× PBS to generate solutions containing approximately 10^{10}, 10^9, 10^8, 10^7, 10^6, 10^5, 10^4, or 10^3 cells/ml. Then 5 µl aliquots of these bacterial solutions (approximately 5×10^7 to 5 cells) were spotted onto LB agar plates supplemented with the appropriate antibiotic (to select for the presence of the plasmid) and either 0 or 50 µM isopropyl ß-D-1-thiogalactopyranoside (IPTG) and incubated overnight at 37 °C. Pictures of the plates were captured using an Amersham Imager 680, and prepared for presentation (cropping representative serial dilutions and adjusting brightness and contrast to facilitate visualization) using Fiji/ImageJ. Each experiment included three biological replicates and at least two experiments were performed; representative data sets are shown.

Long-Term Propagations of Polymorphic Populations

The CFP-tagged sensitive (either WT or Δ*rnhA*) and the five YFP-labeled-resistant bacteria (either RpsL^{K43N}, RpsL^{K43T}, RpoB^{H526L}, RpoB^{H526Y}, and RpoB^{S531F} or Δ*rnhA* RpsL^{K43N}, Δ*rnhA* RpsL^{K43T}, Δ*rnhA* RpoB^{H526L}, Δ*rnhA* RpoB^{H526Y}, and Δ*rnhA* RpoB^{S531F}) were streaked individually onto LB agar plates and incubated overnight at 37 °C. The next day, three independent colonies from each strain were inoculated separately in LB (150 µl per well) in a 96-well plate and incubated overnight at 37 °C with shaking (700 rpm). The next day, bacteria were quantified by Flow Cytometry, and 10 µl of 1:1:1:1:1:1 mixtures of the sensitive and either resistant bacteria were added to 140 µl of medium, at an initial number of approximately 10^6 cells. The initial frequencies of the fluorescent strains were confirmed by Flow Cytometry. Every 24 h, during 15 days, bacterial cultures were diluted in fresh LB and allowed to grow for additional 24 h, reaching approximately 10^9 cells/ml. For the propagations with strong bottleneck (1:1,500 dilutions), cultures were diluted in 1× PBS by a factor of 10^{-2}, and then 10 µl of these diluted cultures were transferred to 140 µl fresh LB. For the propagations with mild bottleneck (1:50 dilutions), 3 µl of bacterial culture were transferred to 147 µl fresh LB. In parallel, cell numbers were counted using the Flow Cytometer, in order to measure the frequency of each strain in the mixed population during the experiment, by collecting a sample (10 µl) from the spent culture each day.

Growth Curves

In the experiments involving RHI001, YFP-tagged sensitive and RpsL^{K43N} RpoB^{H526Y} strains were streaked individually onto LB agar plates and incubated overnight at 37 °C. The next day, three independent colonies from each strain were inoculated separately in LB (150 µl per well) in a 96-well plate and incubated overnight at 37 °C with shaking (700 rpm). The next day, bacteria were quantified by Flow Cytometry, and approximately 5×10^5 bacteria were inoculated in 100-well plates containing LB supplemented with either 0.5% DMSO (the solvent of RHI001) or 50 µM RHI001 (150 µl per well), and incubated at 37 °C with continuous shaking (medium amplitude, duration 5 s, 10 s interval, and stopping 5 s before each measurement) in a Bioscreen C (Oy Growth Curves Ab Ltd.) benchtop microplate reader, measuring OD_{600} every 30 min during 12 h. In the experiments involving sensitive and RpsL^{K43N} RpoB^{H526Y} strains carrying the expression vector pCA24N -gfp, either empty or carrying the gene *dksA* (Kitagawa et al. 2005), the strains were streaked individually onto LB agar plates supplemented with the appropriate antibiotic (to select for the presence of the plasmid), and incubated overnight at 37 °C. The next day, three independent colonies from each strain were inoculated separately in LB supplemented with the appropriate antibiotic (150 µl per well) in a 96-well plate and incubated overnight at 37 °C with shaking (700 rpm). The next day, the OD_{600} of the overnight cultures was measured using a Thermo Scientific Multiskan Go spectrophotometer, bacteria were appropriately diluted in 1× PBS, and approximately 5×10^5 bacteria were inoculated in flat-bottom 96-well plates containing LB (150 µl per well) supplemented with the appropriate antibiotic and either 0 or 50 µM IPTG, and incubated at 37 °C (1 °C up to bottom gradient, "lid on" option) with double orbital shaking (set as "fast") in a Biotek SYNERGY H1 benchtop microplate reader, measuring OD_{600} every 30 min during 24 h.

Animal Experiments

Adult C57BL/6J female mice (6–8 weeks old) were kept in ventilated cages under specified pathogen-free (SPF) barrier conditions at the animal facility of the IGC. To overcome bacterial colonization resistance, mice were treated with streptomycin (5 g/l) in drinking water during 7 days and then put on regular autoclaved water for 2 days to wash out the antibiotic from the intestine. The following day, animals were deprived of food and water during the 4 h prior to inoculation by oral gavage of 100 µl of bacterial suspension containing $\sim 10^9$ cells. All animals were then individually caged, with food and water being available ad libitum. Each animal (six per group) was gavaged with a mix (1:9 ratio) of CFP-tagged sensitive (either WT or Δ*rnhA*) and YFP-labeled double-resistant bacteria (either $RpsL^{K43T}$ $RpoB^{H526Y}$ or Δ*rnhA* $RpsL^{K43T}$ $RpoB^{H526Y}$). In order to obtain the bacterial suspensions, the strains were streaked individually onto appropriate antibiotic-supplemented LB agar plates and incubated overnight at 37 °C. The next day, three independent colonies from each strain were inoculated separately in assay tubes containing 5 ml of BHI broth supplemented with the appropriate antibiotic and bacterial cultures were grown overnight at 37 °C with shaking (240 rpm). The next day, each bacterial culture was diluted 100-fold (20 µl of overnight culture in 2 ml of fresh BHI broth, in 125 ml flasks) and incubated at 37 °C with shaking (240 rpm) until reaching an $OD_{600} \approx 2$. Then the cultures were washed once with 1× PBS and Flow cytometry was used to assess the appropriate cells numbers and prepare bacterial mixes for gavage. Mouse fecal pellets were collected at 8 h after gavage, and afterward on a daily basis during 13 days, to analyze the loads and frequency of each strain colonizing the gut along time. Fecal samples were stored in 15% glycerol at −80 °C. In order to measure the loads (CFUs/g of feces) and the frequency of each strain along the experiment, fecal samples were plated on appropriate antibiotic-supplemented plates and incubated overnight to assess CFUs of CFP- or YFP-labeled bacteria using a SteREOLumar Carl Zeiss fluorescent stereoscope. Every strain that remained below the detection limit ($\sim 10^2$ CFUs/g of feces) for three consecutive time points was considered extinct. For the postgavage antibiotic treatment, streptomycin (5 g/l) was dispensed in drinking water during 7 days. The animal experiments included in this work were reviewed and approved by both the Ethics Committee and the Animal Welfare Body of the IGC (license A009.2018) and by the Direção Geral de Alimentação e Veterinária (DGAV, Portuguese national entity that regulates the use of laboratory animals; license 009676). All experiments conducted on animals followed the Portuguese (Decreto-Lei No. 113/2013) and European (Directive 2010/63/EU) legislations concerning housing, husbandry, and animal welfare.

Measurement of Protein Synthesis Dynamics

Fluorescence intensity of bacteria growing exponentially in LB and carrying an inducible fluorescent chromosomal reporter was measured over the time upon induction (every 20 min during 2 h) by flow cytometry. At every time point, bacterial cultures were appropriately diluted in prewarmed medium in order to maintain the cells in exponential phase. The experiment included the same genotypes carrying the reporter but either never exposed or constantly exposed to the inducer, as negative and positive controls, respectively. These controls were used to calculate the percentage of expression over the time in each genotype.

Statistical Analyses

All analyses were conducted using Libreoffice Calc version 5.4.1.2 (www.libreoffice.org, last accessed April 3, 2021) software, R version 3.4.4 (www.r-project.org, last accessed April 3, 2021) software via RStudio version 1.1.442 interface (www.rstudio.com, last accessed April 3, 2021) and GraphPad Prism version 7.04 (www.graphpad.com, last accessed April 3, 2021). For each set of competitions ($n \geq 3$), one-sample two-tailed Student's *t*-tests were used to determine whether the data set corresponding to each genotype is significantly different than 0 (for fitness cost) or 1 (for SOS induction). For comparing different conditions or genotypes, two-tailed unpaired Student's *t*-tests were used. For testing the association between the fitness cost and the level of SOS induction, the averages of the selection coefficient (s) and the fold change in SOS induction were calculated for each genotype, and these mean values were used to calculate the linear regression of the selection coefficient with the natural logarithm of the fold change in SOS induction.

Supplementary Material

Supplementary data are available at *Molecular Biology and Evolution* online.

Acknowledgments

The authors thank Professor Susan M. Rosenberg and Dr Christian J. Rudolph for kindly providing bacterial strains, the Flow Cytometry and Advanced Imaging facilities of Instituto Gulbenkian de Ciência for technical assistance, Miguel Godinho for useful discussions, and Jonathan Howard, Karina Xavier, Leonardo Gastón Guilgur, Pol Nadal Jiménez, and the members of the Gordo and Xavier labs for critically reading earlier versions of this manuscript. This work was supported by the Marie Sklodowska-Curie Actions (MSCA) with the fellowship 746690-ResistEpist-H2020-MSCA-IF-2016/H2020-MSCA-IF-2016, to R.B., and partially supported by the PREPARE project (JPIAMR/0001/2016-ERA NET), and by ONEIDA and Congento projects (LISBOA-01-0145-FEDER-016417 and LISBOA-01-0145-FEDER-022170), both cofunded by FEEI—"Fundos Europeus Estruturais e de Investimento" from "Programa Operacional Regional Lisboa 2020," and by national funds from "Fundação para a Ciência e a Tecnologia" (FCT), to I.G. R.B. was also supported by the FCT with the fellowship SFRH/BDP/109517/2015. The authors declare no conflicts of interest.

Author Contributions

R.B: conceptualization, formal analysis, funding acquisition, investigation, methodology, visualization, writing—original draft, writing—review and editing. N.F: formal analysis,

investigation, methodology, writing—review and editing. I.G: conceptualization, formal analysis, funding acquisition, methodology, project administration, resources, supervision, writing—review and editing.

Data Availability

All the strains used (supplementary data S1, Supplementary Material online) are available via Material Transfer Agreement (MTA). The raw data of the experiments shown in all figures and the table are available in supplementary data S2, Supplementary Material online. The images analyzed to obtain the data shown in table 1, and those used in supplementary figures S2 and S5, Supplementary Material online, are available in the public data repository Zenodo (doi:10.5281/zenodo.3381746).

References

Almeida Da Silva PEA, Palomino JC. 2011. Molecular basis and mechanisms of drug resistance in *Mycobacterium tuberculosis*: classical and new drugs. *J Antimicrob Chemother*. 66(7):1417–1430.

Andersson DI, Balaban NQ, Baquero F, Courvalin P, Glaser P, Gophna U, Kishony R, Molin S, Tønjum T. 2020. Antibiotic resistance: turning evolutionary principles into clinical reality. *FEMS Microbiol Rev*. 44(2):171–188.

Andersson DI, Hughes D. 2010. Antibiotic resistance and its cost: is it possible to reverse resistance? *Nat Rev Microbiol*. 8(4):260–271.

Andersson DI, Levin BR. 1999. The biological cost of antibiotic resistance. *Curr Opin Microbiol*. 2(5):489–493.

Applebee MK, Herrgård MJ, Palsson BØ. 2008. Impact of individual mutations on increased fitness in adaptively evolved strains of *Escherichia coli*. *J Bacteriol*. 190(14):5087–5094.

Balbontín R, Vlamakis H, Kolter R. 2014. Mutualistic interaction between *Salmonella enterica* and *Aspergillus niger* and its effects on *Zea mays* colonization. *Microb Biotechnol*. 7(6):589–600.

Baquero F, Coque TM, de la Cruz F. 2011. Ecology and evolution as targets: the need for novel eco-evo drugs and strategies to fight antibiotic resistance. *Antimicrob Agents Chemother*. 55(8):3649–3660.

Bertani G. 1951. Studies on lysogenesis. I. The mode of phage liberation by lysogenic *Escherichia coli*. *J Bacteriol*. 62(3):293–300.

Birge EA, Kurland CG. 1969. Altered ribosomal protein in streptomycin-dependent *Escherichia coli*. *Science* 166(3910):1282–1284.

Blattner FR, Plunkett G, Bloch CA, Perna NT, Burland V, Riley M, Collado-Vides J, Glasner JD, Rode CK, Mayhew GF, et al. 1997. The complete genome sequence of *Escherichia coli* K-12. *Science* 277(5331):1453–1462.

Bohman K, Ruusala T, Jelenc PC, Kurland CG. 1984. Kinetic impairment of restrictive streptomycin-resistant ribosomes. *Mol Gen Genet*. 198(2):90–99.

Broccoli S, Rallu F, Sanscartier P, Cerritelli SM, Crouch RJ, Drolet M. 2004. Effects of RNA polymerase modifications on transcription-induced negative supercoiling and associated R-loop formation. *Mol Microbiol*. 52(6):1769–1779.

Burmann BM, Schweimer K, Luo X, Wahl MC, Stitt BL, Gottesman ME, Rösch P. 2010. A NusE: nusG complex links transcription and translation. *Science* 328(5977):501–504.

Chittum HS, Champney WS. 1994. Ribosomal protein gene sequence changes in erythromycin-resistant mutants of *Escherichia coli*. *J Bacteriol*. 176(20):6192–6198.

Crossley MP, Bocek M, Cimprich KA. 2019. R-loops as cellular regulators and genomic threats. *Mol Cell*. 73(3):398–411.

Das A, Merril C, Adhya S. 1978. Interaction of RNA polymerase and *rho* in transcription termination: coupled ATPase. *Proc Natl Acad Sci U S A*. 75(10):4828–4832.

Datsenko KA, Wanner BL. 2000. One-step inactivation of chromosomal genes in *Escherichia coli* K-12 using PCR products. *Proc Natl Acad Sci U S A*. 97(12):6640–6645.

Dong H, Kurland CG. 1995. Ribosome mutants with altered accuracy translate with reduced processivity. *J Mol Biol*. 248(3):551–561.

Durão P, Balbontín R, Gordo I. 2018. Evolutionary mechanisms shaping the maintenance of antibiotic resistance. *Trends Microbiol*. 26(8):677–691.

Durão P, Trindade S, Sousa A, Gordo I. 2015. Multiple resistance at no cost: rifampicin and streptomycin a dangerous Liaison in the spread of antibiotic resistance. *Mol Biol Evol*. 32(10):2675–2680.

Dutta D, Shatalin K, Epshtein V, Gottesman ME, Nudler E. 2011. Linking RNA polymerase backtracking to genome instability in *E. coli*. *Cell* 146(4):533–543.

Elgamal S, Artsimovitch I, Ibba M. 2016. Maintenance of transcription-translation coupling by elongation factor P. *mBio* 7(5).

Eliopoulos GM. 1993. Aminoglycoside resistant enterococcal endocarditis. *Infect Dis Clin North Am*. 7(1):117–133.

Figueroa-Bossi N, Bossi L. 2015. Recombineering applications for the mutational analysis of bacterial RNA-binding proteins and their sites of action. *Methods Mol Biol Clifton Biol*. 1259:103–116.

Fisher RF, Yanofsky C. 1983. Mutations of the beta subunit of RNA polymerase alter both transcription pausing and transcription termination in the *trp* operon leader region *in vitro*. *J Biol Chem*. 258(13):8146–8150.

Galas DJ, Branscomb EW. 1976. Ribosome slowed by mutation to streptomycin resistance. *Nature* 262(5569):617–619.

Gan W, Guan Z, Liu J, Gui T, Shen K, Manley JL, Li X. 2011. R-loop-mediated genomic instability is caused by impairment of replication fork progression. *Genes Dev*. 25(19):2041–2056.

Gartner TK, Orias E. 1966. Effects of mutations to streptomycin resistance on the rate of translation of mutant genetic information. *J Bacteriol*. 91(3):1021–1028.

Goldstein BP. 2014. Resistance to rifampicin: a review. *J Antibiot*. 67(9):625–630.

Gorini L, Kataja E. 1964. Streptomycin-induced oversuppression in *E. coli*. *Proc Natl Acad Sci U S A*. 51:995–1001.

Gowrishankar J, Pittard J. 1982. Regulation of phenylalanine biosynthesis in *Escherichia coli* K-12: control of transcription of the *pheA* operon. *J Bacteriol*. 150(3):1130–1137.

Guarente LP, Beckwith J. 1978. Mutant RNA polymerase of *Escherichia coli* terminates transcription in strains making defective *rho* factor. *Proc Natl Acad Sci U S A*. 75(1):294–297.

Gupta R, Chatterjee D, Glickman MS, Shuman S. 2017. Division of labor among *Mycobacterium smegmatis* RNase H enzymes: RNase H1 activity of RnhA or RnhC is essential for growth whereas RnhB and RnhA guard against killing by hydrogen peroxide in stationary phase. *Nucleic Acids Res*. 45(1):1–14.

Hall AR, Iles JC, MacLean RC. 2011. The fitness cost of rifampicin resistance in *Pseudomonas aeruginosa* depends on demand for RNA polymerase. *Genetics* 187(3):817–822.

Hammer K, Jensen KF, Poulsen P, Oppenheim AB, Gottesman M. 1987. Isolation of *Escherichia coli rpoB* mutants resistant to killing by lambda cII protein and altered in *pyrE* gene attenuation. *J Bacteriol*. 169(11):5289–5297.

Herbert KM, Zhou J, Mooney RA, Porta AL, Landick R, Block SM. 2010. *E. coli* NusG inhibits backtracking and accelerates pause-free transcription by promoting forward translocation of RNA polymerase. *J Mol Biol*. 399(1):17–30.

Hershberg R. 2017. Antibiotic-independent adaptive effects of antibiotic resistance mutations. *Trends Genet*. 33(8):521–528.

Hosaka T, Tamehiro N, Chumpolkulwong N, Hori-Takemoto C, Shirouzu M, Yokoyama S, Ochi K. 2004. The novel mutation K87E in ribosomal protein S12 enhances protein synthesis activity during the late growth phase in *Escherichia coli*. *Mol Genet Genomics*. 271(3):317–324.

Jensen KF. 1988. Hyper-regulation of *pyr* gene expression in *Escherichia coli* cells with slow ribosomes. Evidence for RNA polymerase pausing *in vivo*? *Eur J Biochem*. 175(3):587–593.

Jin DJ, Cashel M, Friedman DI, Nakamura Y, Walter WA, Gross CA. 1988. Effects of rifampicin resistant *rpoB* mutations on antitermination and interaction with *nusA* in *Escherichia coli*. *J Mol Biol*. 204(2):247–261.

Jin DJ, Gross CA. 1989. Characterization of the pleiotropic phenotypes of rifampin-resistant *rpoB* mutants of *Escherichia coli*. *J Bacteriol*. 171(9):5229–5231.

Jin DJ, Gross CA. 1991. RpoB8, a rifampicin-resistant termination-proficient RNA polymerase, has an increased Km for purine nucleotides during transcription elongation. *J Biol Chem*. 266(22):14478–14485.

Jin DJ, Walter WA, Gross CA. 1988. Characterization of the termination phenotypes of rifampicin-resistant mutants. *J Mol Biol*. 202(2):245–253.

Jin DJ, Zhou YN. 1996. Mutational analysis of structure-function relationship of RNA polymerase in *Escherichia coli*. *Methods Enzymol*. 273:300–319.

Katz S, Hershberg R. 2013. Elevated mutagenesis does not explain the increased frequency of antibiotic resistant mutants in starved aging colonies. *PLoS Genet*. 9(11):e1003968.

Kim J, Yoon J, Ju M, Lee Y, Kim T-H, Kim J, Sommer P, No Z, Cechetto J, Han S-J. 2013. Identification of two HIV inhibitors that also inhibit human RNaseH2. *Mol Cells*. 36(3):212–218.

Kitagawa M, Ara T, Arifuzzaman M, Ioka-Nakamichi T, Inamoto E, Toyonaga H, Mori H. 2005. Complete set of ORF clones of *Escherichia coli* ASKA library (a complete set of *E. coli* K-12 ORF archive): unique resources for biological research. *DNA Res Int Res*. 12(5):291–299.

Kogoma T. 1997. Stable DNA replication: interplay between DNA replication, homologous recombination, and transcription. *Microbiol Mol Biol Rev*. 61(2):212–238.

Kohler R, Mooney RA, Mills DJ, Landick R, Cramer P. 2017. Architecture of a transcribing-translating expressome. *Science* 356(6334):194–197.

Lang KS, Hall AN, Merrikh CN, Ragheb M, Tabakh H, Pollock AJ, Woodward JJ, Dreifus JE, Merrikh H. 2017. Replication-transcription conflicts generate R-loops that orchestrate bacterial stress survival and pathogenesis. *Cell* 170(4):787–799.e18.

Lemos ACM, Matos ED. ED. 2013. Multidrug-resistant tuberculosis. *Braz J Infect Dis off Dis*. 17(2):239–246.

Lennox ES. 1955. Transduction of linked genetic characters of the host by bacteriophage P1. *Virology* 1(2):190–206.

Leónidas Cardoso L, Durão P, Amicone M, Gordo I. 2020. Dysbiosis individualizes the fitness effect of antibiotic resistance in the mammalian gut. *Nat Ecol Evol*. 4(9):1268–1278.

Li X-T, Thomason LC, Sawitzke JA, Costantino N, Court DL. 2013. Positive and negative selection using the *tetA-sacB* cassette: recombineering and P1 transduction in *Escherichia coli*. *Nucleic Acids Res*. 41(22):e204.

Lin LL, Little JW. 1988. Isolation and characterization of noncleavable (Ind-) mutants of the LexA repressor of *Escherichia coli* K-12. *J Bacteriol*. 170(5):2163–2173.

Maslowska KH, Makiela-Dzbenska K, Fijalkowska IJ. 2019. The SOS system: a complex and tightly regulated response to DNA damage. *Environ Mol Mutagen*. 60(4):368–384.

McMahon G, Landau JV. 1982. Effect of S12 ribosomal mutations on peptide chain elongation in *Escherichia coli*: a hydrostatic pressure study. *J Bacteriol*. 151(1):516–520.

Melnyk AH, Wong A, Kassen R. 2015. The fitness costs of antibiotic resistance mutations. *Evol Appl*. 8(3):273–283.

Merrikh H, Machón C, Grainger WH, Grossman AD, Soultanas P. 2011. Co-directional replication-transcription conflicts lead to replication restart. *Nature* 470(7335):554–557.

Merrikh H, Zhang Y, Grossman AD, Wang JD. 2012. Replication-transcription conflicts in bacteria. *Nat Rev Microbiol*. 10(7):449–458.

Minias AE, Brzostek AM, Korycka-Machala M, Dziadek B, Minias P, Rajagopalan M, Madiraju M, Dziadek J. 2015. RNase HI is essential for survival of *Mycobacterium smegmatis*. *PLoS One* 10(5):e0126260.

Moura de Sousa J, Balbontín R, Durão P, Gordo I. 2017. Multidrug-resistant bacteria compensate for the epistasis between resistances. *PLoS Biol*. 15(4):e2001741.

Murphy KC, Campellone KG, Poteete AR. 2000. PCR-mediated gene replacement in *Escherichia coli*. *Gene* 246(1–2):321–330.

Myka KK, Gottesman ME. 2019. DksA and DNA double-strand break repair. *Curr Genet*. 65(6):1297–1300.

Myka KK, Küsters K, Washburn R, Gottesman ME. 2019. DksA-RNA polymerase interactions support new origin formation and DNA repair in *Escherichia coli*. *Mol Microbiol*. 111(5):1382–1397.

Negro V, Krin E, Aguilar Pierlé S, Chaze T, Giai Gianetto Q, Kennedy SP, Matondo M, Mazel D, Baharoglu Z. 2019. RadD contributes to R-loop avoidance in sub-MIC tobramycin. *mBio* 10(4).

Neidhardt FC, Curtiss R, Ingraham JL, Lin ECC, Low KB, Magasanik B, Reznikoff W, Riley M, Schaechter M, Umbarger HE. 1996. Escherichia coli and Salmonella: cellular and molecular biology. Washington (DC): ASM Press.

Ochi K, Hosaka T. 2013. New strategies for drug discovery: activation of silent or weakly expressed microbial gene clusters. *Appl Microbiol Biotechnol*. 97(1):87–98.

Ozaki M, Mizushima S, Nomura M. 1969. Identification and functional characterization of the protein controlled by the streptomycin-resistant locus in *E. coli*. *Nature* 222(5191):333–339.

Paulander W, Maisnier-Patin S, Andersson DI. 2009. The fitness cost of streptomycin resistance depends on *rpsL* mutation, carbon source and RpoS (sigmaS). *Genetics* 183(2):539–546.

Pelchovich G, Nadejda S, Dana A, Tuller T, Bravo IG, Gophna U. 2014. Ribosomal mutations affecting the translation of genes that use non-optimal codons. *FEBS J*. 281(16):3701–3718.

Proshkin S, Rahmouni AR, Mironov A, Nudler E. 2010. Cooperation between translating ribosomes and RNA polymerase in transcription elongation. *Science* 328(5977):504–508.

Qi Q, Preston GM, MacLean RC. 2014. Linking system-wide impacts of RNA polymerase mutations to the fitness cost of rifampin resistance in *Pseudomonas aeruginosa*. *mBio* 5(6):e01562.

Quillardet P, Huisman O, D'Ari R, Hofnung M. 1982. SOS chromotest, a direct assay of induction of an SOS function in *Escherichia coli* K-12 to measure genotoxicity. *Proc Natl Acad Sci U S A*. 79(19):5971–5975.

Quiñones A, Kücherer C, Piechocki R, Messer W. 1987. Reduced transcription of the *rnh* gene in *Escherichia coli* mutants expressing the SOS regulon constitutively. *Mol Gen Genet*. 206(1):95–100.

Reynolds MG. 2000. Compensatory evolution in rifampin-resistant *Escherichia coli*. *Genetics* 156(4):1471–1481.

Ruusala T, Andersson D, Ehrenberg M, Kurland CG. 1984. Hyper-accurate ribosomes inhibit growth. *EMBO J*. 3(11):2575–2580.

Sambrook J, Fritsch EF, Maniatis T. 1989. .Molecular cloning: a laboratory manual. New York: CSHL Press.

Saxena S, Myka KK, Washburn R, Costantino N, Court DL, Gottesman ME. 2018. *Escherichia coli* transcription factor NusG binds to 70S ribosomes. *Mol Microbiol*. 108(5):495–504.

Schrag SJ, Perrot V. 1996. Reducing antibiotic resistance. *Nature* 381(6578):120–121.

Sedlyarova N, Rescheneder P, Magán A, Popitsch N, Rziha N, Bilusic I, Epshtein V, Zimmermann B, Lybecker M, Sedlyarov V, et al. 2017. Natural RNA polymerase aptamers regulate transcription in *E. coli*. *Mol Cell*. 67(1):30–43.e6.

Shee C, Cox BD, Gu F, Luengas EM, Joshi MC, Chiu L-Y, Magnan D, Halliday JA, Frisch RL, Gibson JL, et al. 2013. Engineered proteins detect spontaneous DNA breakage in human and bacterial cells. *Elife* 2:e01222.

Skarstad K, Løbner-Olesen A, Atlung T, von Meyenburg K, Boye E. 1989. Initiation of DNA replication in *Escherichia coli* after overproduction of the DnaA protein. *Mol Gen Genet*. 218(1):50–56.

Sousa A, Frazão N, Ramiro RS, Gordo I. 2017. Evolution of commensal bacteria in the intestinal tract of mice. *Curr Opin Microbiol*. 38:114–121.

Stockum A, Lloyd RG, Rudolph CJ. 2012. On the viability of *Escherichia coli* cells lacking DNA topoisomerase I. *BMC Microbiol*. 12:26.

Subramaniam AR, Pan T, Cluzel P. 2013. Environmental perturbations lift the degeneracy of the genetic code to regulate protein levels in bacteria. *Proc Natl Acad Sci U S A*. 110(6):2419–2424.

Tadokoro T, Kanaya S. 2009. Ribonuclease H: molecular diversities, substrate binding domains, and catalytic mechanism of the prokaryotic enzymes. *FEBS J*. 276(6):1482–1493.

Tehranchi AK, Blankschien MD, Zhang Y, Halliday JA, Srivatsan A, Peng J, Herman C, Wang JD. 2010. The transcription factor DksA prevents conflicts between DNA replication and transcription machinery. *Cell* 141(4):595–605.

Thomas M, White RL, Davis RW. 1976. Hybridization of RNA to double-stranded DNA: formation of R-loops. *Proc Natl Acad Sci U S A*. 73(7):2294–2298.

Tramontano E, Corona A, Menendez-Arias L. 2019. Ribonuclease H, an unexploited target for antiviral intervention against HIV and hepatitis B virus. *Antiviral Res*. 171:104613.

Trindade S, Sousa A, Gordo I. 2012. Antibiotic resistance and stress in the light of Fisher's model. *Evolution* 66(12):3815–3824.

Trindade S, Sousa A, Xavier KB, Dionisio F, Ferreira MG, Gordo I. 2009. Positive epistasis drives the acquisition of multidrug resistance. *PLoS Genet*. 5(7):e1000578.

Vogwill T, MacLean RC. 2015. The genetic basis of the fitness costs of antimicrobial resistance: a meta-analysis approach. *Evol Appl*. 8(3):284–295.

Wang CH, Koch AL. 1978. Constancy of growth on simple and complex media. *J Bacteriol*. 136(3):969–975.

Wimberly H, Shee C, Thornton PC, Sivaramakrishnan P, Rosenberg SM, Hastings PJ. 2013. R-loops and nicks initiate DNA breakage and genome instability in non-growing *Escherichia coli*. *Nat Commun*. 4:2115.

World Health Organization. 2018. Global antimicrobial resistance surveillance system (GLASS) report: early implementation 2017-2018. Geneva: World Health Organization.

Wrande M, Roth JR, Hughes D. 2008. Accumulation of mutants in "aging" bacterial colonies is due to growth under selection, not stress-induced mutagenesis. *Proc Natl Acad Sci U S A*. 105(33):11863–11868.

Yanofsky C, Horn V. 1981. Rifampin resistance mutations that alter the efficiency of transcription termination at the tryptophan operon attenuator. *J Bacteriol*. 145(3):1334–1341.

Yu D, Ellis HM, Lee EC, Jenkins NA, Copeland NG, Court DL. 2000. An efficient recombination system for chromosome engineering in *Escherichia coli*. *Proc Natl Acad Sci U S A*. 97(11):5978–5983.

Zaman S, Fitzpatrick M, Lindahl L, Zengel J. 2007. Novel mutations in ribosomal proteins L4 and L22 that confer erythromycin resistance in *Escherichia coli*. *Mol Microbiol*. 66(4):1039–1050.

Zhou YN, Jin DJ. 1997. RNA polymerase beta mutations have reduced sigma70 synthesis leading to a hyper-temperature-sensitive phenotype of a sigma70 mutant. *J Bacteriol*. 179(13):4292–4298.

Zhou YN, Jin DJ. 1998. The *rpoB* mutants destabilizing initiation complexes at stringently controlled promoters behave like "stringent" RNA polymerases in *Escherichia coli*. *Proc Natl Acad Sci U S A*. 95(6):2908–2913.

Zhou YN, Lubkowska L, Hui M, Court C, Chen S, Court DL, Strathern J, Jin DJ, Kashlev M. 2013. Isolation and characterization of RNA polymerase *rpoB* mutations that alter transcription slippage during elongation in *Escherichia coli*. *J Biol Chem*. 288(4):2700–2710.